

Carl A. Mears*, Matthias C. Schabel, and Frank J. Wentz
Remote Sensing Systems

1. INTRODUCTION

Researchers in the global change community generally agree on the presence of surface warming observed over the past century (Hansen et al. 2001; Houghton et al. 2001). In the middle troposphere, the situation is less clear due to the paucity of long term, stable observations. Radiosondes, the principal tool for atmospheric profiling, have limited spatial coverage, particularly over large portions of the oceans, and are subject to a host of complications including changing instrument types, configurations, and observing practices. The advent of temperature sounding microwave radiometers flown on NOAA polar orbiting weather satellites has provided a new and complementary source of upper atmosphere observations beginning with TIROS-N in 1978 and continuing through the present, the nine Microwave Sounding Units (MSU), and the follow-on instruments, the Advanced Microwave Sounding Units (AMSU). These instruments were designed and calibrated primarily for meteorological rather than climatological purposes. Despite excellent coverage (more than half the earth's surface daily for each instrument), the MSU data suffer from a number of calibration issues and time-varying biases which must be characterized and removed if MSU are to be used for climate change studies.

Christy and Spencer (Christy et al. 2000) have discovered a number of important sources of error in those data, including intersatellite offsets, the significance of slowly evolving diurnal sampling, and significant correlation between observed intersatellite brightness temperature differences and satellite hot calibration load temperatures. This previous work has played a controversial, high-profile role in the debate over the presence and origin of tropospheric warming. In the light of the importance of these data in the formulation of policy decisions, we have performed an entirely separate, end-to-end analysis of the middle/upper tropospheric (channel 2) data from the nine satellites MSU series of instruments. Our philosophy differs from that of Christy and Spencer in that all satellite overlaps are given equal weight, as opposed to using a "backbone" formed from some satellite pairs, and ignoring others (Christy et al. 2000). We also avoid the spatial smoothing and interpolation procedures that Spencer and Christy perform in order to produce their monthly anomaly products (Spencer and Christy 1992).

The MSU instruments are cross-track scanning microwave radiometers which measure the upwelling

microwave radiance for 11 views with corresponding incidence angles ranging from -56 to 56 degrees, with the center view, view 6, making a nadir measurement. MSU channel 2, at 53.74 GHz, measures thermal emission from molecular oxygen in a thick layer of the atmosphere, with the peak contribution coming from near 7 km, but with significant contributions coming from the surface through the lower stratosphere. The measured radiance serves as a proxy for mid-and-upper tropospheric temperature, since it is unlikely that the emission properties of the troposphere in this frequency band, which are due mostly to oxygen, are changing significantly over the time period of this study.

2. ADJUSTMENTS MADE PRIOR TO MERGING

Before we can begin to study intersatellite differences, we must first remove a number of sources of long term drift and bias from the data. The two most important of these are correction of the incidence angles, with errors due to orbital decay and an apparent satellite attitude bias (Wentz and Schabel 1998; Mears et al. 2002), and effects due to evolution each instrument's local measurement time, which aliases the local diurnal cycle into the long term record (Christy et al. 2000).

While examining long-term averages of cross-scan brightness temperature differences, we found a systematic bias that can be modeled as an approximately constant bias in incidence angle consistent with an instrument roll error. This roll, in conjunction with information about the satellite height, allows us to adjust each measurement to correspond to the nadir view. Adjusting to nadir reduces noise when measurement from different fields of view are combined to produce average observations.

The removal of the diurnal sampling effect is more complicated. Spencer and Christy used averages of cross-scan bias, with the constant bias mentioned above removed by comparing ascending and descending orbital nodes, to deduce the local diurnal

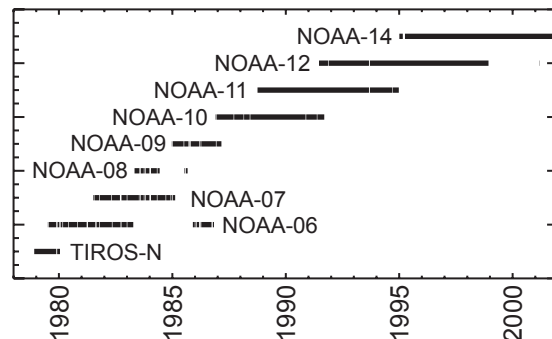


Figure 1. Period of valid channel 2 data for each of the 9 MSU instruments.

* Corresponding Author Address: Carl A. Mears, Remote Sensing Systems, 438 First Street Suite 200, Santa Rosa, CA, 95401. Email: mears@remss.com

slope for a zonal band. This method is too noisy to accurately remove the diurnal cycle for each grid point separately. We instead use a modeled brightness temperature climatology calculated using 5 years of hourly CCM3 (Kiehl et al. 1996) output to adjust each measurement to local noon (Mears et al. 2002). Our diurnal climatology is validated by comparing it to morning/evening differences in actual MSU measurements (Mears et al. 2002).

3. INTERSATELLITE MERGING PROCEDURE

After performing the above adjustments and a number of quality control procedures (Mears et al. 2002), we then need to account for systematic differences between the satellites. Intersatellite calibration is performed by studying measurements made by co-orbiting instruments. In Fig. 1, we show the operating period for each of the 9 instruments. Each instrument

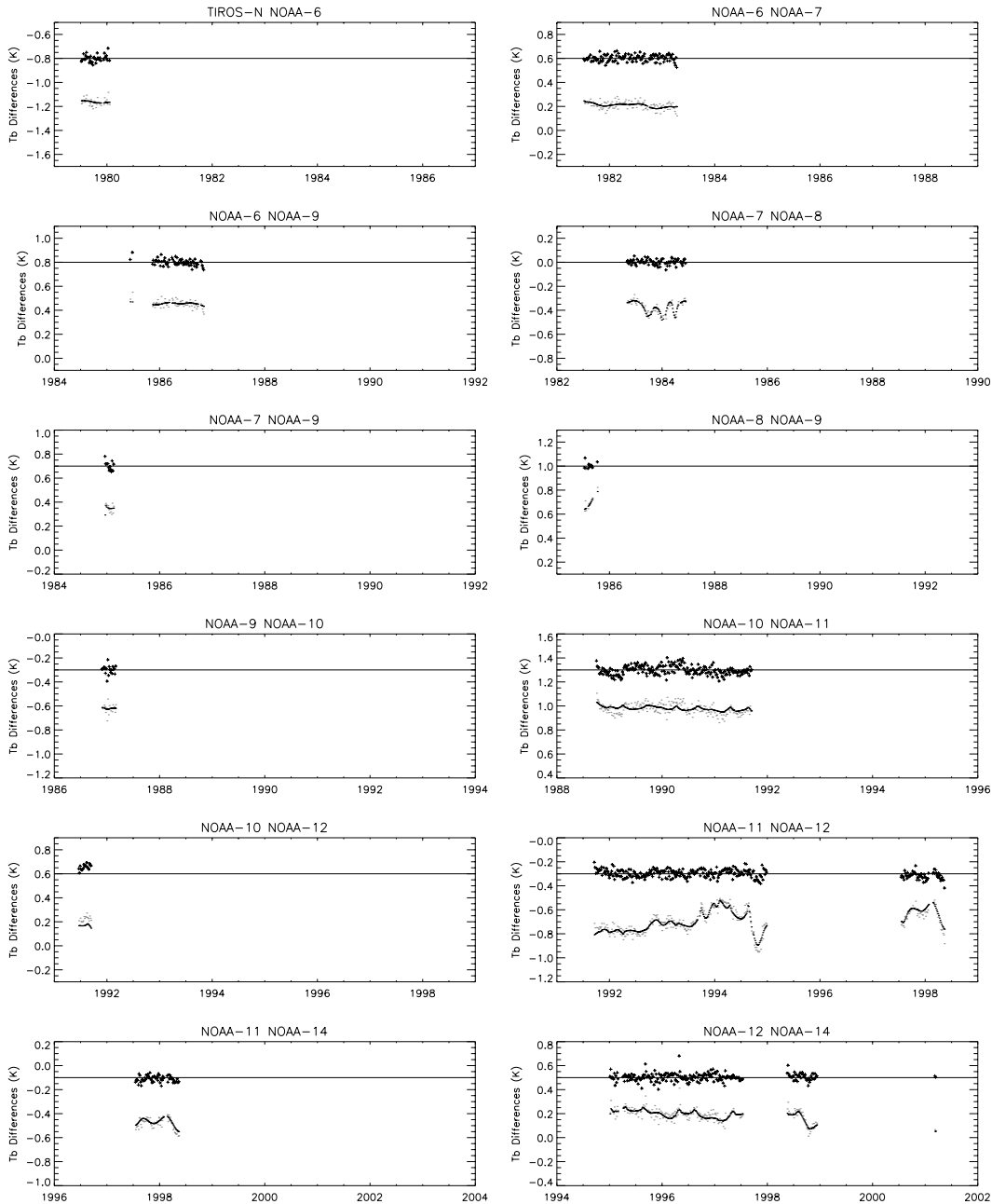


Figure 2. Results of the satellite merging calculation, plotted separately for each satellite pair. In each plot, gray dots represent oceanic pentad averages of brightness temperature differences between pairs of satellites, and the black dots are a fit to the differences, using only both constant satellite offsets and target factors. The black crosses are the residuals to the fit, offset for clarity. The line through the black crosses is a horizontal line at zero residual to guide the eye.

typically overlaps with one or more other instruments allowing complete, transitive, intercalibration of the nine instruments. We shall see later that the long term calibration of the set is critically dependent on the NOAA-09/NOAA-10 overlap, which is only 90 days long. We form pentad (five-day) global average time series for each satellite for the entire globe using the central five views, as well as global averages for the land-only and ocean-only geographical subsets. When contemporaneous pentads from different satellites are compared, the differences are well explained an error model containing both intersatellite offsets, and a term proportional to the calibration target temperature anomaly, which we believe is necessary due to unresolved errors in the measurement and subsequent removal of radiometer nonlinearities. As will be discussed below, this effect makes a large contribution to the overall error budget of the inter-satellite merging procedure. The error model for brightness temperature is

$$T_{MEAS,i} = T_0 + A_i + \alpha_i T_{TARGET,i} + \varepsilon_i \quad (1)$$

where T_0 is the true brightness temperature, A_i is the temperature offset for the i -th instrument, α_i is a small multiplicative “target factor” describing the correlation of the measured temperature with the temperature of the hot calibration target, $T_{TARGET,i}$ is the target temperature anomaly for the i -th satellite, and ε_i is an error term that contains additional zero-mean errors due to instrumental noise and sampling effects. For any contemporaneous pair of pentads, we can difference two instances of Eq. 1 to obtain.

$$T_{diff}(t_n) = T_{MEAS,i}(t_n) - T_{MEAS,j}(t_n) = A_i + \alpha_i T_{TARGET,i}(t_n) - A_j - \alpha_j T_{TARGET,j}(t_n) + \varepsilon_i - \varepsilon_j, \quad (2)$$

Here t_n represents the time of the given pentads. The set of all such equations for each valid pentad overlap between 2 or more satellites (with care being taken to avoid linearly dependent equations that can arise for

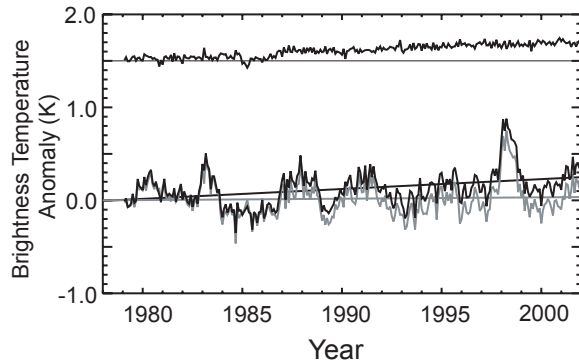


Figure 3. Global time series of MSU Channel 2 brightness temperature. The low black line is our time series, and the gray line is that found by Christy and Spencer. The upper black line is the difference time series.

instances where 3 satellites are operating simultaneously) form a set of many (~1200) equations in 17 unknowns (nine target factors (α_i) and eight offsets (A_i). $A_{NOAA-10}$ is arbitrarily set to zero to avoid a singular set of equations. This system can then be solved using a least-squares linear regression technique, where the sum of the squared differences between satellite measurements are minimized, yielding the best fit merging parameters.

In Figure 2 we show the results of this regression for the ocean-only pentads. We use the ocean only merge results to fix the α 's, since the ocean measurements are less likely to be affected by diurnal effects not removed by our diurnal climatology. We plot the intersatellite differences, the regressed fit to the differences, and the after-the-fit residuals for each satellite pair. It is clear from the figure that the target temperature dependence is essential for a good fit – without this term, the fitting functions would be constant in time and would not remove the seasonal scale variations in the differences.

We use the α 's from the ocean only merge to perform a global, land-and-ocean merge, where new values for the offsets are calculated to minimize the intersatellite differences. These new offsets are within 0.04 of the ocean only offsets – these differences are likely due to the different zonal sampling in the more inclusive data set. We combine the adjusted pentads into a single time series, which is then resampled onto a monthly time scale to facilitate comparison with Christy and Spencer's earlier results.

4. RESULTS

We show the results of the merging procedure in Figure 3. On a short time scale, our results are almost identical to those of Christy and Spencer, but on a longer time scale, we show significantly (0.1K/decade)

Table I. Summary of Decadal Trend Results

	Analysis Method	Trend (K/Decade)
Ocean-only	Diurnally corrected	0.098 +/- 0.018
	No diurnal correction	0.091 +/- 0.020
	Spencer and Christy	-0.011
Land-only	Diurnally corrected	0.087 +/- 0.030
	No diurnal correction	0.023 +/- 0.030
	Spencer and Christy	0.050
Global	Diurnally corrected	0.097 +/- 0.020
	No diurnal correction	0.067 +/- 0.020
	Spencer and Christy	0.009

more warming. A significant difference occurs during the 1985-1987 time period, during the lifetime of NOAA-09, where we see a $\sim 0.1\text{K}$ ramp in the difference between our respective time series. We summarize our decadal trend for each geographical subset in the table below. We also include results found when the diurnal adjustment is not performed, and the trends found using Christy and Spencer's data for the same geographical subset. In all three cases, our trends are significantly warmer than those found by Christy and Spencer, though the difference is less than 0.03K per decade for land-only results. The diurnal correction has only a small effect on our ocean-only results supporting our use of ocean-only observations to determine the target factors.

When we compare our values of the target factors with those used by Christy and Spencer, we find good agreement for all values except for NOAA-09. Both sets of target factors are plotted in Figure 4, below. In order to quantify the effect of the differing NOAA-09 target multipliers, we exactly reproduced our ocean-only merging procedure with the sole exception that we used the CS target factors. The resulting global trend obtained was 0.014 K/decade , a value much closer to Christy and Spencer's value of -0.011 K/decade than our fully corrected value of 0.099 K/decade . Similarly, if we use our target factors, except that we fix the value of the NOAA-9 target factor to the CS value of 0.095 , the trend value becomes 0.022 K/decade , indicating that differences in this one target factor are responsible for a large fraction of the overall difference between these analyses.

To produce gridded global maps of brightness temperature trend, we use the ocean-only target factors and the land-and-ocean offsets derived above to merged time series of daily observations on a $2.5\text{ degree} \times 2.5\text{ degree}$ latitude and longitude grid, again using only the central five views. The resulting merged time series is resampled into a monthly time series, and

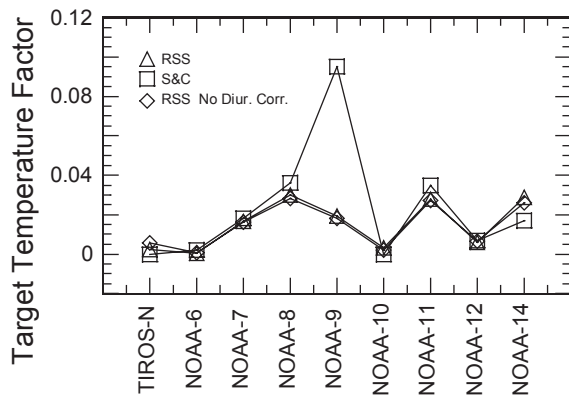


Figure 4. Comparison of target temperature factors. The two sets of RSS derived target temperature factors were calculated using ocean-only data. The Christy and Spencer target temperature factors were obtained using both land and ocean data. Note the general agreement between the RSS values and the C&S values, except for NOAA-09.

a resulting trend is calculated for each point. In Figure 5, we show color-coded maps of decadal trends for our data, and a trend map calculated using the same method, except using the Christy and Spencer data available on the web.

Both the RSS and CS trend maps show significant warming in the northern hemisphere, and their zonal profiles seem quite similar in shape despite the global trend offset of 0.1 K/decade . However, examination of the zonal difference map in Fig. 13c reveals a strong latitude-dependence of the offset, with a clear upward step between 30N and the Equator, which is also clearly mirrored in the global trend difference map. In the high northern latitudes where large regions of significant warming over Siberia and northeastern Canada are observed, and where the vast majority of high quality radiosonde observations used in validations of the CS data set reside, the two data sets are in generally good agreement, both in terms of the characteristic spatial patterns and in absolute trend magnitude. Two notable

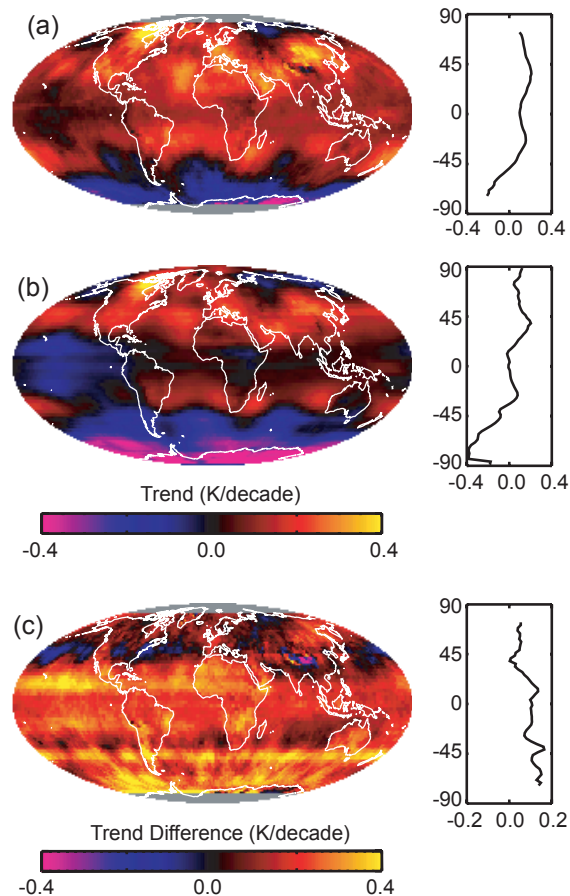


Figure 5. Color-coded map of global MSU channel 2 brightness temperature trends for the period 1979-2001 for the RSS (a) and CS (b) data sets. The spatial distribution of trend differences (RSS-CS) is plotted on the same scale in (c).

exceptions are over northern Africa, where we observe significant warming relative to CS, and the Himalayas, where we see much less warming than CS. In both of these cases, the final trend will be quite sensitive to details of the diurnal temperature correction. The tropics and southern high latitudes, in contrast, show significant biases between the RSS data and the CS data. Both data sets reveal significant cooling in the southern oceans and over Antarctica, but the magnitude of this is much smaller in our analysis.

5. ACKNOWLEDGEMENTS

This work was performed under the auspices of the NOAA Climate and Global Change Program and the Joint NOAA/NASA Enhanced Data Set Project.

6. REFERENCES

- Christy, J. R., R. W. Spencer, et al. (2000). "MSU Tropospheric Temperatures: Dataset Construction and Radiosonde Comparisons." *Journal of Atmospheric and Oceanic Technology* **17**(9): 1153-1170.
- Hansen, J. E., R. Ruedy, et al. (2001). "A Closer look at United States and global surface temperature change." *J. Geophys. Res.* **106**: 23947-23963.

- Houghton, J. T., Y. Ding, et al., Eds. (2001). *Climate Change 2001: The Scientific Basis: Contribution of Working Group I to the Third Assessment Report of the Intergovernmental Panel on Climate Change*. Cambridge, UK, Cambridge University Press.
- Kiehl, J. T., J. J. Hack, et al. (1996). Description of the NCAR Community Climate Model (CCM3). Boulder: National Center for Atmospheric Research.
- Mears, C. A., M. Schabel, et al. (2002). "Correcting the MSU Middle Tropospheric Temperature for Diurnal Drifts." *Proceedings of the International Geophysics and Remote Sensing Symposium III*: 1839-1841.
- Mears, C. A., M. C. Schabel, et al. (2002). "A Reanalysis of the MSU Channel 2 Tropospheric Temperature Record." Submitted to *J. Clim.*
- Spencer, R. W. and J. R. Christy (1992). "Precision and Radiosonde Validation of Satellite Gridpoint Temperature Anomalies. Part I: MSU Channel 2." *Journal of Climate* **5**: 847-857.
- Wentz, F. J. and M. Schabel (1998). "Effects of satellite orbital decay on MSU lower tropospheric temperature trends." *Nature* **394**: 661-664.